Performance improvement of inverted polymer solar cells using quantum dots and nanorod array

Ching-Ting Lee[1,2,3] · Hsin-Ying Lee[2] · Hsuch-Chih Hsu[3]

Abstract

Due to the high absorption at short wavelength and the color conversion effect, CdSe/ZnS core–shell quantum dots were blended into poly (3-hexylthiophene):[6,6]-phenyl-C_{61}-butyric acid methyl ester (P3HT:PCBM) as an active layer of invert polymer solar cells (IPSCs). Compared with the IPSCs using P3HT:PCBM active layer, the short-circuit current density was improved from 10.38 to 11.57 mA/cm^2 and the power conversion efficiency was improved from 3.37 to 3.73% for the IPSCs using P3HT:PCBM:CdSe/ZnS active layer. Since the carrier mobility of organic materials is very small, the carrier collection ability is limited by the short carrier transport length before they are recombined. Therefore, the power conversion efficiency of the resulting organic solar cells is unavoidably restricted by the low carrier collection ability. In this work, to improve carrier collection ability, indium tin oxide (ITO) nanorod array was embedded. Compared with the short-circuit current density of 11.57 mA/cm^2 and the power conversion efficiency of 3.73% of the IPSCs using P3HT:PCBM:CdSe/ZnS active layer, the short-circuit current density of 15.60 mA/cm^2 and the power conversion efficiency of 4.86% were obtained for the IPSCs by embedding 1.0 µm periodic ITO nanorod array in the P3HT:PCBM:CdSe/ZnS active layer.

1 Introduction

In the past years, because of environment pollution and energy shortage, various green renewable energy sources are urgently researched and developed. Among them, solar energy sources have been substantially attracted and focused as the mainstream product and dominate market due to their sufficiency and nonpollution [1]. In general, the solar energy sources include silicon-based solar cells [2, 3], III–V-based solar cells [4, 5], and organic solar cells [6–9]. In view of the inherent advantages of flexibility, simple fabrication, large area, and light weight, organic solar cells have especially drawn lots of attention, recently. In the traditional structure of organic solar cells, polymer material, poly (3,4-ethylene-dioxythiophene):poly (styrene sulfonate) (PEDOT:PSS), aluminum (Al), and indium tin oxide (ITO) were used as active layer, hole transport layer (HTL), cathode electrode, and anode electrode, respectively. However, because of the corrosive electrode and the vulnerable reaction of active layer with oxygen, the traditional structure has critical problems of low stability and low power conversion efficiency (PCE) [10–12]. To overcome those drawbacks, an inverted structure of polymer solar cells was designed, a high work function metal (e.g. Ag or Au) was used to replace Al, and alumina-doped zinc oxide (AZO) or cesium carbonate (Cs_2CO_3) was used to replace PEDOT:PSS [13, 14]. Recently, several methods were proposed to enhance the performances of organic solar cells by doping appropriate materials in the active layer and using embedded nanostructure [15, 16]. However, the PCE of those resulting organic solar cells was still not acceptable due to the low light absorption at short wavelength and the imperfect carrier collection. In this work, to improve performances, an ITO nanorod array was embedded to enhance carrier collection and CdSe/ZnS core–shell quantum dots were blended in poly (3-hexylthiophene):[6,6]-phenyl-C_{61}-butyric acid methyl ester (P3HT:PCBM) active layer to enhance short wavelength absorption, simultaneously. To optimize the structure of ITO nanorod array, various periods were patterned using a He–Cd laser interference photolithography

✉ Ching-Ting Lee
    ctlee@ee.ncku.edu.tw

1   Department of Electrical Engineering, Yuan Ze University, Taoyuan 320, Taiwan, ROC

2   Department of Photonics, National Cheng Kung University, Tainan 701, Taiwan, ROC

3   Institute of Microelectronics, Department of Electrical Engineering, National Cheng Kung University, Tainan 701, Taiwan, ROC

method. Furthermore, various contents of CdSe/ZnS quantum dots were blended into P3HT:PCBM active layer to study the optimal content of the CdSe/ZnS quantum dots.

2 Experiments

Figure 1 illustrates the schematic configuration of inverted polymer solar cells (IPSCs) with ITO nanorod array and blended CdSe/ZnS quantum dots. A photoresist was spread on a 300-nm-thick ITO-coated polyethylene terephthalate (PET) substrate using a spin coater. An interference grating was performed using the two-beam He–Cd laser interference photolithography system [17]. Afterwards, the sample was exposed again by rotating an angle of 90° using the same process parameters. By changing the intersection angle
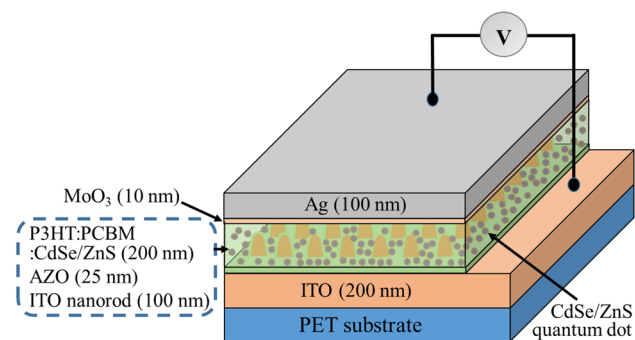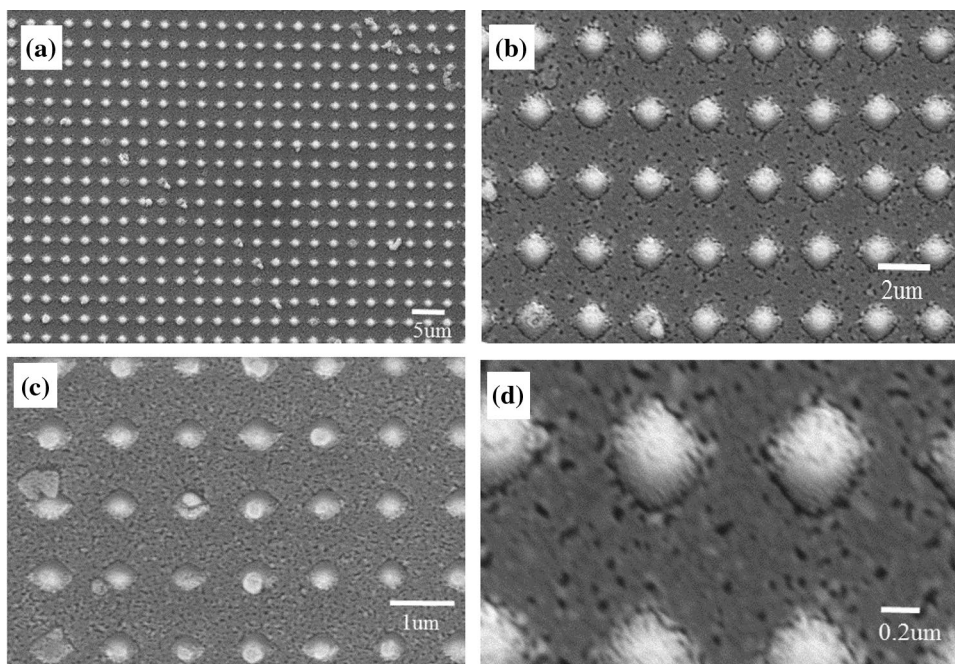

Fig. 1 Schematic configuration of inverted polymer solar cells with ITO nanorod array and blended CdSe/ZnS quantum dots

of the two-beam He–Cd laser, various periodic photoresist patterns could be obtained. After developing in developer solution for 30 s and then etching in chemical solution of HCl:deionized water (25:75) for 15 min, various dimensional ITO nanorod arrays with a height of 100 nm were formed. The scanning electron microscope images of the fabricated ITO nanorod arrays with a period of 3.0, 2.0, 1.0, and 0.5 μm were shown in Fig. 2a–d, respectively. A 25-nm-thick AZO film was then deposited as an electron transportation layer (ETL) using a radio frequency magnetron sputtering system. Using Hall measurement, the electron concentration and the electron mobility of the AZO film were 8.1×10^{19} cm^{-3} and 3.1 cm^2/V-s, respectively. Subsequently, after mixing 1,2-dichloribenzene (DCB) with blended various CdSe/ZnS core–shell quantum dots, P3HT (20 mg) and PCBM (16 mg), various 200-nm-thick P3HT:PCBM:CdSe/ZnS active layers were respectively formed by spin-coating the prepared solution on the AZO films. The samples were then annealed in a nitrogen glove box at 110 °C for 20 min. Finally, a 10-nm-thick MoO$_3$ layer and a 100-nm-thick Ag layer were subsequently deposited as hole transportation layer (HTL) and anode electrode using a thermal coater. The dimension of the IPSCs was 4 mm^2.

3 Experimental results and discussion

Using the measurement of UV–VIS spectrometer (Hitachi U4100), the absorption spectra of the various P3HT:PCBM:CdSe/ZnS active layers were shown in Fig. 3. Because the absorption at the shorter wavelength increased
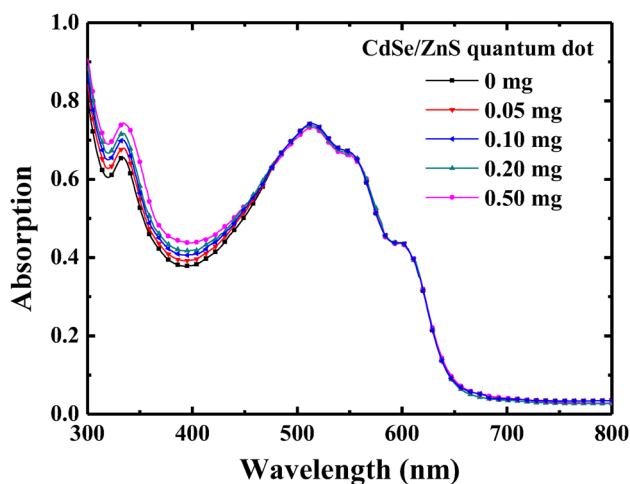
Fig. 2 Scanning electron microscope images of ITO nanorod array with a period of **a** 3.0 μm, **b** 2.0 μm, **c** 1.0 μm and **d** 0.5 μm

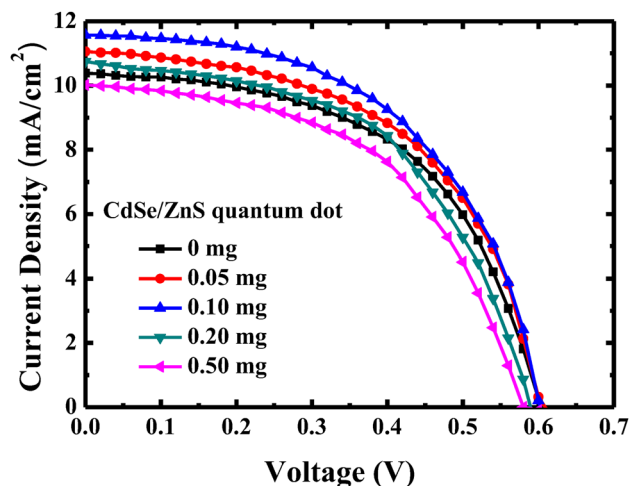**Fig. 3** Absorption spectra of various P3HT:PCBM:CdSe/ZnS layers

Fig. 4 Current density–voltage characteristics of inverted polymer solar cells without ITO nanorod array and with various CdSe/ZnS quantum dots

Table 1 Photovoltaic characteristics of IPSCs with various CdSe/ZnS quantum dots

Quantum dots (mg)	V_{oc} (V)	J_{sc} (mA/cm^2)	FF (%)	PCE (%)
0	0.60	10.38	54.1	3.37
0.05	0.60	11.06	53.8	3.57
0.10	0.60	11.57	53.7	3.73
0.20	0.59	10.75	53.2	3.37
0.50	0.58	10.02	52.5	3.05

Fig. 5 External quantum efficiency of inverted polymer solar cells with various CdSe/ZnS quantum dots

with an increase of the CdSe/ZnS content in the active layer, it was verified that the light absorption would be improved by blending CdSe/ZnS quantum dots in the P3HT:PCBM films.

The current density–voltage (J–V) characteristics of the IPSCs were measured at a room temperature using a J–V curve tracer under an illumination of 100 mW/cm^2 with an AM 1.5G solar simulator. Figure 4 shows the J–V characteristics of the IPSCs without ITO nanorod array and with various contents of CdSe/ZnS quantum dots in the P3HT:PCBM:CdSe/ZnS active layers. Table 1 listed the photovoltaic characteristics of short-circuit current density (J_{sc}), open-circuit voltage (V_{oc}), fill factor (FF), and PCE. It was found that the PCE increased with an increase of CdSe/ZnS quantum dots until 0.1 mg and then decreased

by blending more CdSe/ZnS quantum dots. Among the various inverted polymer solar cells, the best PCE of 3.73% was obtained by using 0.10 mg CdSe/ZnS quantum dot in the P3HT:PCBM:CdSe/ZnS active layers. To investigate the mechanisms of the PCE as a function of the content of CdSe/ZnS quantum dots, the external quantum efficiency (EQE) as a function of wavelength was measured using a chopper with lock-in amplifier for phase-sensitive detection and using a xenon lamp as light source. Figure 5 shows the dependent EQE on the wavelength of the various inverted polymer solar cells. It was found that the changing tendency of the J_{sc} was the same as the external quantum efficiency. In general, the PCE was influenced by the light absorption and the carrier mobility in the active layer of solar cells. Although the light absorption in the shorter wavelength was enhanced with an increase of CdSe/ZnS quantum dots in the P3HT:PCBM:CdSe/ZnS active layer as shown in Fig. 3, the best PCE of 3.73% was obtained by using the 0.10 mg CdSe/ZnS quantum dots. To study the mechanisms, the dark current density as a function of voltage was measured and shown in Fig. 6. It was found that the dark current density
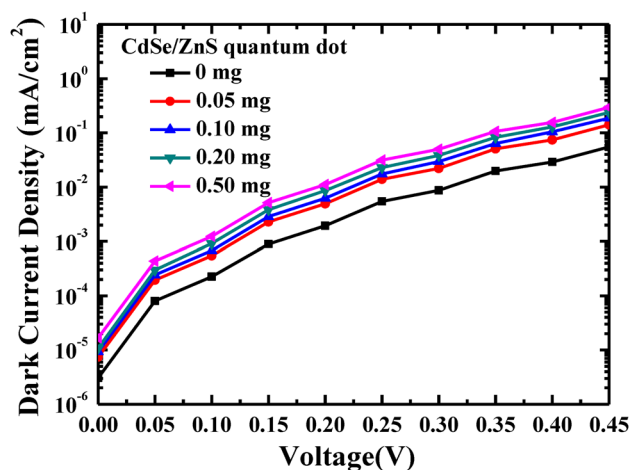
Fig. 6 Dark current density–voltage characteristics of inverted polymer solar cells with various CdSe/ZnS quantum dots

Fig. 7 Current density–voltage characteristics of inverted polymer solar cells with various periodic ITO nanorod arrays by blending 0.10 mg CdSe/ZnS quantum dots in active layers

increased with an increase of the content of CdSe/ZnS quantum dot in the active layer. This phenomenon was attributed to the segregating effect by blending more CdSe/ZnS quantum dots in the P3HT:PCBM:CdSe/ZnS active layer. Consequently, the associated V_{oc} and FF were reduced. Therefore, the largest short-circuit current density of 11.57 mA/cm^2 was obtained by using 0.10 mg CdSe/ZnS quantum dots in the active layer. Therefore, the IPSCs using 0.10 mg CdSe/ZnS quantum dots could exhibit the largest J_{sc} of 11.57 mA/cm^2 and the best PCE of 3.73%.

To study the enhanced photovoltaic performance of nanorod array, Fig. 7 shows the J–V characteristics of the IPSCs with various periodic ITO nanorod arrays using 0.10 mg CdSe/ZnS quantum dots in the P3HT:PCBM:CdSe/ZnS active layers. The associated photovoltaic characteristics are listed in Table 2. Since the carrier mobility in the active layer was small, the transport length would be short before they were recombined. Therefore, the carrier collection would be improved by using the narrower periodic ITO nanorod array. Consequently, the J_{sc} increased by reducing the period of the ITO nanorod array as listed in Table 2. Compared with the J_{sc} of 11.57 mA/cm^2 of the IPSCs without ITO nanorod array, the J_{sc} was enhanced to 15.62 mA/cm^2 by using 0.5 μm periodic ITO nanorod array. The EQE as a function of wavelength of the IPSCs with various periodic ITO nanorod arrays were measured and shown in Fig. 8. It was found that both the EQE and the J_{sc} increased with a reduction of the period of the ITO nanorod array. To study the dependence of V_{oc} and FF on the period of ITO nanorod arrays, the dark current density of the various IPSCs was measured and shown in Fig. 9. It was found that the dark current density increased by reducing the period of the ITO nanorod array due to the induced more defects on the surface of the tinier ITO nanorods caused by the chemical etching
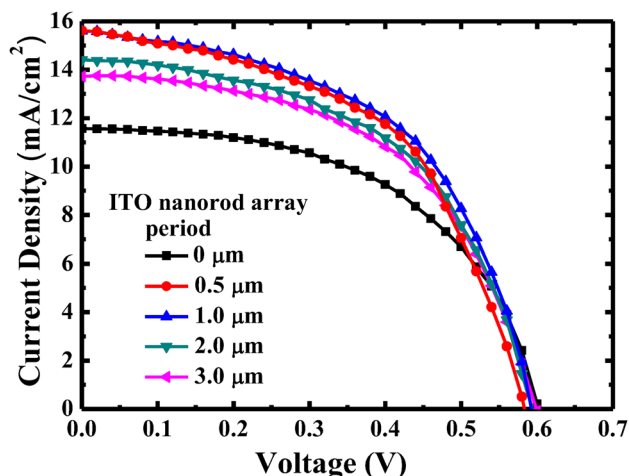
Table 2 Photovoltaic characteristics of IPSCs with various periodic ITO nanorod arrays

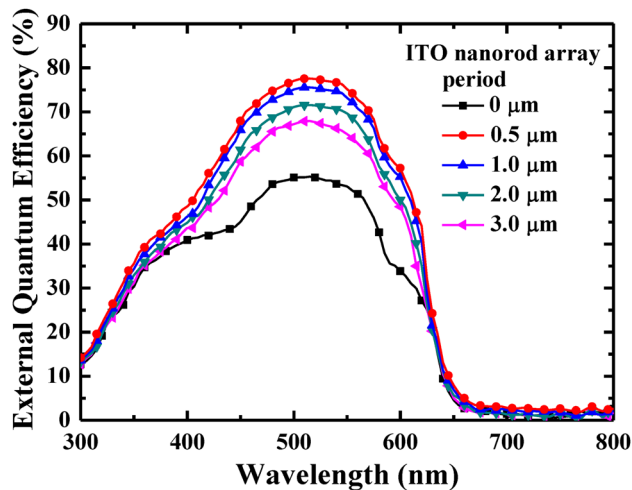| Period (μm)	V_{oc} (V)	J_{sc} (mA/cm^2)	FF (%)	PCE (%)
0	0.60	11.57	53.7	3.73
0.5	0.58	15.62	51.9	4.69
1.0	0.59	15.60	52.8	4.86
2.0	0.59	14.40	53.1	4.51
3.0	0.60	13.72	53.4	4.40

Fig. 8 External quantum efficiency of inverted polymer solar cells with various periodic ITO nanorod arrays by blending 0.10 mg CdSe/ZnS quantum dots in active layers
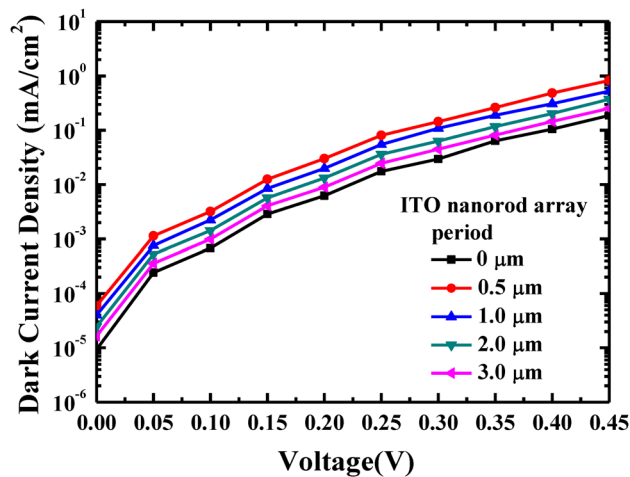
Fig. 9 Dark current density- voltage characteristics of inverted polymer solar cells with various periodic ITO nanorod arrays by blending 0.10 mg CdSe/ZnS quantum dots in active layers

process. Therefore, the V_{oc} and FF were gradually degraded with a decrease of the period of ITO nanorod arrays. By trading off the V_{oc}, J_{sc}, and FF, the best PCE of 4.86% was obtained by using 1.0 μm periodic ITO nanorod array.

4 Conclusions

In this study, the photovoltaic characteristics of IPSCs with various CdSe/ZnS quantum dots in P3HT:PCBM:CdSe/ZnS active layers and various periodic ITO nanorod arrays fabricated on PET flexible substrates were studied. The light absorption at the shorter wavelength of the P3HT:PCBM:CdSe/ZnS active layer could be enhanced by blending more CdSe/ZnS quantum dots. However, the segregating effect would be induced by blending over CdSe/ZnS quantum dots. Consequently, the best J_{sc} and EQE were obtained by blending 0.10 mg CdSe/ZnS quantum dots in P3HT:PCBM:CdSe/ZnS active layers. Furthermore, compared with the IPSCs using P3HT:PCBM active layer, the PCE was improved from 3.37 to 3.73% by blending 0.10 mg CdSe/ZnS quantum dots in P3HT:PCBM:CdSe/ZnS active layers. Furthermore, in view of the inherent disadvantage of small mobility of organic materials, the PCE of the resulting solar cells would be low. The low PCE was attributed to the low carrier collection ability, because the carrier transport length was short before they were recombined. To enhance the carrier collection ability, ITO nanorod array was embedded. The J_{sc} of the IPSCs was increased by reducing the period of ITO nanorod array. Compared with the J_{sc} of 11.57 mA/cm² of the planar IPSCs without ITO nanorod array, the J_{sc} was improved to 15.60 mA/cm² by using 1.0 μm periodic ITO nanorod array. Consequently, the PCE was improved from 3.73 to 4.86%. It is well known that the performances of IPSCs is highly determined by the quality of the organic materials. In this work, to focus and demonstrate the proposed CdSe/ZnS quantum dots and ITO nanorod array in active layers, the general marked organic materials were used in the IPSCs.

References

1. K.W.J. Barnham, M. Mazzer, B. Clive, Nat. Mater. **5**, 161 (2006)
2. J. Schmidt, R. Peibst, R. Brendel, Sol. Energy Mater. Sol. Cells **187**, 39 (2018)
3. V. Titova, J. Schmidt, AIP Adv. **8**, 125023 (2018)
4. J.W. Boucher, A.L. Greenaway, K.E. Egelhofer, S.W. Boettcher, Sol. Energy Mater. Sol. Cells **159**, 546 (2017)
5. S. Pouladi, M. Rathi, D. Khatiwada, M. Asadirad, S.K. Oh, P. Dutta, Y. Yao, Y. Gao, S. Sun, Y. Li, S. Shervin, K.H. Lee, V. Selvamanickam, J.H. Ryou, Prog. Photovolt. Res. Appl. **27**, 30 (2019)
6. C.T. Lee, C.H. Lee, Org. Electron. **14**, 2046 (2013)
7. G.S. Chen, Y.C. Chen, C.T. Lee, H.Y. Lee, Sol. Energy **174**, 897 (2018)
8. E.L. Lim, C.C. Yap, M.H.H. Jumali, F.L. Khairulaman, J. Mater. Sci. **30**, 2726 (2019)
9. T. Soga, S. Kato, S. Kato, N. Kishi, J. Mater. Sci. **30**, 3332 (2019)
10. J.Y. Oh, M. Shin, H.W. Lee, Y.J. Lee, H.K. Baik, U. Jeong, ACS Appl. Mater. Interfaces **6**, 7759 (2014)
11. X.W. Guo, Y.X. Zhang, X.J. Liu, S. Braun, Z.Q. Wang, B. Li, Y.Q. Li, C.G. Duan, M. Fahlman, J.X. Tang, J.F. Fang, Q.Y. Bao, Org. Electron. **59**, 15 (2018)
12. M. Elshobaki, J. Anderegg, S. Chaudhary, ACS Appl. Mater. Interfaces **6**, 12196 (2014)
13. H.L. Huang, C.T. Lee, H.Y. Lee, Org. Electron. **21**, 126 (2015)
14. G. Li, C.W. Chu, V. Shrotriya, J. Huang, Y. Yang, Appl. Phys. Lett. **88**, 253503 (2006)
15. S.H. Wang, Y.J. Hsiao, T.H. Fang, M.H. Lin, S.H. Kanga, ECS J. Solid State Sci. Technol. **2**, M52 (2013)
16. X.M. He, F. Gao, G.L. Tu, D. Hasko, S. Hüttner, U. Steiner, N.C. Greenham, R.H. Friend, W.T.S. Huck, Nano Lett. **10**, 1302 (2010)
17. C.T. Lee, H.Y. Juo, IEEE J. Electron Devices Soc. **6**, 183 (2018)